Hybrid Control in Automotive Applications: the Cut-off Control.

A. Balluchi [a], M.D. Di Benedetto [b], C. Pinello [a], C. Rossi [c] and A. Sangiovanni–Vincentelli [a,d]

[a] *PARADES, Via San Pantaleo, 66, 00186 Roma, Italy*

[b] *Dipartimento di Ingegneria Elettrica, Università dell'Aquila, Poggio di Roio, 67040 L'Aquila, Italy*

[c] *Magneti Marelli S.p.A., Via del Timavo, 33, 40134 Bologna, Italy*

[d] *Department of Electrical Engineering and Computer Science, University of California at Berkeley, CA 94720, USA*

Abstract

A novel approach to the control of an automotive engine in the cut-off region is presented. First, a hybrid model which describes the torque generation mechanism and the powertrain dynamics is developed. Then, the cut-off control problem is formulated as a hybrid optimal control problem, whose solution is obtained by relaxing it to the continuous domain and mapping its solution back into the hybrid domain. A formal analysis as well as experimental results demonstrate the properties and the quality of the control law.

1 Introduction

Hybrid systems have been the subject of intensive study in the past few years with particular emphasis placed on a unified representation of the models in terms of rigorous mathematical foundations (see [11], [16], [14], [13], [7], [8]). The class of hybrid control problems is extremely broad since it obviously contains continuous control problems as well as discrete event control problems as special cases. For this reason, it is very difficult to devise a general yet effective strategy to solve hybrid control problems. In our opinion, it is important to address significant domains of application of hybrid control to develop further understanding of the implications of the model on the control algorithms.

In this paper, we focus on a domain of application that is of great industrial interest: automotive engine control. In this domain, the ever increasing

computational power of micro–controllers has made it possible to extend the performance and the functionality of electronic sub–systems controlling the motion of the car. This opportunity has exposed the need for control algorithms with guaranteed properties that can reduce substantially emission and gas consumption while maintaining the performance of the car [15,4,11]. We argue that most of the engine control problems are hybrid control problems since the behavior of four–stroke gasoline engines is determined by the combination of a discrete event sub-system modeling the torque generation process, and a continuous time sub-system modeling the powertrain behavior. It is then the plant to be controlled that is hybrid, no matter whether the control strategy is implemented with a digital or analog controller. This is an important point to make since some interesting general approaches to hybrid control assume that the plant to be controlled has a continuous dynamics and hence they are not directly applicable here [12,9,5]. In this paper, we introduce such a hybrid model for the engine and we use it to solve a particular case of engine control problem that is of practical interest: the cut-off management problem. We believe that our approach can be used as a general paradigm for a number of other difficult engine control problems such as, for instance, idle speed control.
Engine behavior is in general partitioned into regions of operation where appropriate control action are applied to yield the desired result [6]. The region of operation considered here is characterized by the driver who, by releasing the gas pedal, requests no torque to the engine. An obvious strategy to minimize gas consumption and emissions when no torque is requested is to shut fuel injection off, an operation called *cut–off*. However, cutting off fuel injection as soon as the gas pedal is released, causes a sudden torque reduction that may result in unpleasant oscillations compromising driving comfort. A more complex control action involves modulating torque from the present value to the value corresponding to cut–off in an attempt to prevent oscillations. This control policy is implemented by slowing down air flow [1] decay and, when air quantity is below a threshold, reducing fuel injection gradually to zero. As is often the case, heuristic rule–based controls need extensive tuning, yield satisfactory solutions only in a limited range of operations and are hardly optimal with respect to the emissions and fuel consumption. In particular this approach suffers from the following drawbacks:

- if air reduction is too slow, when the driver releases the gas pedal and presses the clutch pedal to change gear, engine speed raises for a while, thus causing a definite reduction in passengers' comfort;
- if air and/or fuel reduction is too fast, oscillations take place anyway.

[1] In cars equipped with drive–by–wire, throttle valve actuation allows full air flow regulation. In traditional cars, where this regulation is not available, the throttle valve is directly connected to the gas pedal. The value of the minimum air flow can be set either by idle-speed or by the cut-off control.

The control strategy is open–loop in the sense that the state of the powertrain is not taken into account to decide how to control the engine from its present operating conditions to cut–off and, hence, poor performance and emission control may result.
In this paper, we introduce a novel, theoretically sound, closed–loop approach to cut–off control. The "plant" consists of two parts: the engine responsible for torque generation, modeled as a combination of a Finite State Machine and of a Discrete Event system, and the powertrain modeled as a fourth–order linear Continuous Time system. The goal is to control the evolution of the system from the initial condition (the state of the system when the gas pedal has been released and the manifold pressure has approached its idle regime value) to cut–off, minimizing the amplitude of the undesired oscillations. The idle air controls are set to their maximum, in order to achieve the greatest possible torque. The remaining available control actions are on fuel injection and spark ignition, the inputs to the engine, *occurring only once per engine cycle for each piston*. Note that this synchronization constraint makes the problem particularly complex. The torque generated is the output of the engine and the input to the powertrain. The powertrain dynamics contain the potential oscillatory behavior to be minimized. The wheel revolution speed and the angular velocity of the crankshaft are components of its state. The timing of the torque generation mechanism is determined by the angle of the crankshaft. Consequently, the control problem is a Hybrid System Control problem, which is further complicated by the delay between the time in which the decision on the quantity of fuel to be injected is taken (at the beginning of the exhaust phase) and the time the effect of this decision takes place (during the next expansion phase).

Our approach to the hybrid problem at hand is to relax the problem to the continuous time domain assuming that the torque signal can be modulated continuously over time within a given range of values. The problem so obtained is non trivial since the objective function is non differentiable. We devise a strategy that solves this problem to yield an optimal control law for the continuous time domain. Then, this solution in the continuous domain is mapped back into the hybrid domain. The solution in the hybrid domain is demonstrated to yield a behavior that is close (within a precisely specified bound) to the behavior of the control in the continuous case. Our overall strategy is similar to the one proposed by Nerode et al. in [12,9,5], but the specific techniques are completely different since the plant to be controlled is itself hybrid and there are synchronization constraints on the control inputs that make their approach inapplicable.

Our main contributions are:

- the discrete event model of torque generation;
- the formulation of the control problem as a hybrid optimal control problem;

- a solution to the resulting non differentiable continuous problem;
- a sub-optimal solution to the problem in the hybrid space.

From the application of our control strategy by our industrial partner on a commercial vehicle, the proposed solution appears to be far superior than the present, heuristic approach in performance, emission control, in memory and CPU occupation.

The paper is organized as follows. In Section 2, the torque–generation and powertrain models are presented and the precise formulation of the optimal control problem is offered. In Section 3, an optimal solution to the continuous time relaxed control problem is presented. In Section 4, a hybrid control scheme based on the continuous time approximation is proposed to yield a solution demonstrably close to the upper bounding optimal solution to the relaxed problem. A comparison with the presently used control methods is offered in Section 5.

2 Problem formulation

2.1 Plant model

In this section, the hybrid model proposed in [1][2] for vehicles with 4–stroke N–cylinder gasoline engine is illustrated. The hybrid model $\mathcal{M}_{1cyl}$ of a vehicle with single cylinder engine is reported in Figure 1. This model is composed of three parts:

(1) a Finite State Machine (FSM) [2] describing the behavior of the pistons;
(2) a Discrete Event system (DE) [3] modeling torque generation;
(3) a Continuous Time system (CT) modeling the powertrain.

The combination of the FSM and the DE system describes the torque generation mechanism for a single cylinder, whose behavior is affected by the CT powertrain evolution. The hybrid model for a N-cylinder vehicle is obtained composing N FSM/DE cylinder models and the CT powertrain model.

[2] A deterministic Finite State Machine is a six-tuple $M = \{I, Y, \mathcal{S}, s_0, \lambda, \gamma\}$ where I is the (finite) set of inputs, Y is the (finite) set of outputs, $\mathcal{S}$ is the finite set of states, s_0 is the initial state, $\lambda : \mathcal{S} \times I \to \mathcal{S}$ is the next state function, $\gamma : \mathcal{S} \times I \to Y$ is the output function.
[3] A DE system is intended in the sense of [10].

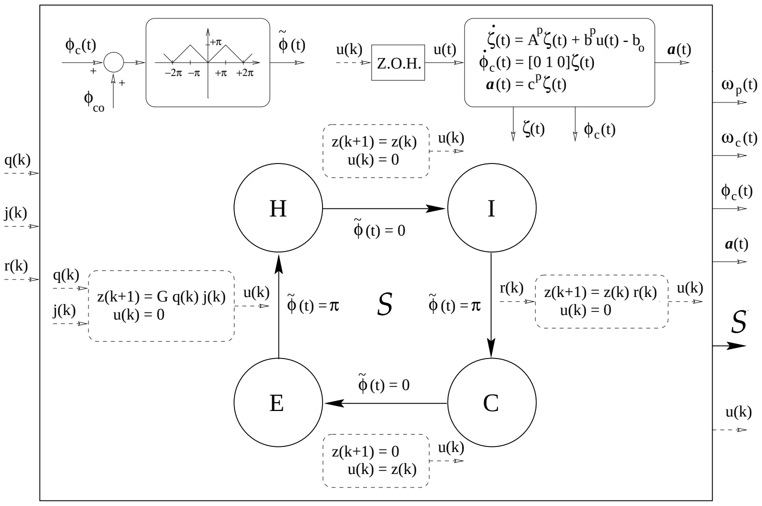

Fig. 1. Hybrid model for a vehicle with 4–stroke single cylinder engine.

Powertrain Model. The powertrain is described by a continuous time system model developed, identified and validated at Magneti Marelli Engine Control Division. Powertrain dynamics are modeled by the linear system

$$\dot{\zeta} = A^p \zeta + b^p u - b_0 \tag{1}$$

$$\dot{\phi}_c = [0,\ 1,\ 0]\ \zeta \tag{2}$$

$$a = c^p \zeta \tag{3}$$

Where $\zeta = [\alpha_e, \omega_c, \omega_p]^T$ represents the axle torsion angle, the crankshaft revolution speed, the wheel revolution speed, and the 4–th variable ϕ_c represents the crankshaft angle. The input signal u is the torque produced by the engine and acting on the crankshaft. Vector b_0 models the resistant actions on the powertrain, due to both internal friction and external forces. Dynamics (1) is asymptotically stable and is characterized by a real dominant pole λ_1, and a pair of conjugate complex poles $\lambda \pm j\mu$. Vehicle acceleration (3) is the powertrain output of interest for drivability and comfort. Assuming vehicle speed equal to wheel speed and denoting by R_w the wheel radius, we have $a = R_w \dot{\omega}_p = R_w[0,0,1]A^p\zeta$. Model parameters A^p, b^p, c^p, and b_0 depend on the transmission gear, and it is assumed that, during a cut–off operation, the driver does not act on the gear.

Cylinder's behavior. The behavior of each cylinder in the engine is abstractly represented by the Finite State Machine shown in Figure 1. FSM state $\mathcal{S}$ assumes values in the set $\{H, I, C, E\}$ as follows.

- *Exhaust run* represented by state H. The piston goes up from the bottom to the top of its run (bottom and top dead centers resp.), expelling combustion exhaust gases.

- *Intake run* represented by state I. During its down–run the piston loads the air–fuel mix.
- *Compression run* represented by state C. During its up movement the piston compresses the loaded mix.
- *Expansion run* represented by state E. The compressed mix combustion, generated by a spark signal, produces a sudden pressure increase which pushes the piston downwards.

The transitions occur when the piston reaches the bottom or top dead center. The guard conditions enabling the transitions in the FSM are written in terms of the piston position expressed by $\tilde{\phi}$: the absolute value of the crank angle with respect to the upper dead center position, related to the crankshaft angle ϕ_c as depicted in Figure 1, where ϕ_{co} corresponds to the angle the crank is mechanically mounted on the shaft.

Torque generation. One remark on the process of torque generation (see [1] [3]) is that the timing of the spark can be set at each cycle in order to modulate the generated torque. Moreover this process is characterized by the delays between the times in which fuel injection and spark advance are set and the time in which such decisions have an effect. Control signals are then subject to a transport process which can be represented by a DE system active at every FSM transition. Such DE system, reported in Figure 1 with dashed boxes, increments its time counter k by one at each transition. Its inputs are: the mass of air-fuel mix $q(k) \in \mathbb{R}^+$ loaded during the intake phase; a binary control variable $j(k) \in \{0, 1\}$ which indicates whether or not the fuel is present in the mix; the modulation factor $r(k) \in [r_{min}, 1]$ due to not optimal spark timing. The DE system output is the torque $u(k)$. At the FSM transition $E \to H$ the DE system reads its inputs $q(k)$ and $j(k)$, and stores in its state $z \in \mathbb{R}$ the maximum amount of torque achievable during the next expansion phase, obtained by the mix-to-torque gain G. Such value is corrected at the $I \to C$ transition applying the modulation factor $r(k)$, due to the chosen spark advance. The DE output $u(k)$ is always zero except at the $C \to E$ transition when it is set to the value stored in z. Input $u(t)$ to the CT powertrain dynamics is obtained from $u(k)$ by a zero order hold block, i.e. between two transitions of the FSM occurring at times t_k and t_{k+1}, it holds $u(t) = u(k)$ for $t \in [t_k, t_{k+1})$.

Engine hybrid model. The overall model of torque generation for a N–cylinder[4] engine is then the combination of N FSMs and of N DE systems representing the behavior of each cylinder as the ones reported in Figure 1.

[4] For example, Formula 1 racing cars can have 8, 10 or 12 cylinders. Fiat Coupè 2000 Turbo has 5.

The hybrid model of the complete vehicle is obtained by adding to torque generation model the powertrain CT dynamics (1),(3). In this paper we focus on the most relevant case of a 4-cylinder engine. Its model, referred to in the rest of the paper as $\mathcal{M}_{4cyl}$, has input signals $\mathbf{j} = [j_1, j_2, j_3, j_4]^T$ and $\mathbf{r} = [r_1, r_2, r_3, r_4]^T$ properly synchronized with the corresponding DE models; we denote by $\mathcal{J}_{4cyl}$ and $\mathcal{R}_{4cyl}$, respectively, the classes of functions $\mathbb{N} \to \{0,1\}^4$ and $\mathbb{N} \to [r_{min}, 1]^4$, feasible for $\mathbf{j}$ and $\mathbf{r}$. Signal q is instead shared among the cylinders. In a 4-cylinder engine at any time each cylinder FSM is in a different state and all transitions are synchronous, that is offset angles ϕ_{c0_i} are either 0 or π. Without loss of generality, we assume that in the model $\mathcal{M}_{4cyl}$ the crankshaft offsets ϕ_{co_i} are $\phi_{c0_1} = \phi_{c0_3} = \pi, \phi_{c0_2} = \phi_{c0_4} = 0$.

2.2 The optimization problem

Inputs to the hybrid engine model $\mathcal{M}_{4cyl}$ are: the mass of air q, fuel injection $\mathbf{j}$ and spark advance modulation factor $\mathbf{r}$. In modern drive–by–wire cars, where the throttle valve is actuated by an electrical motor, the mass of air q is a regulated variable and the designer has full control on the torque generation. For such systems the cut–off problem can be formulated as a fuel minimization problem with comfort as a constraint. We focus on traditional systems, where the throttle valve is directly connected to the gas pedal and there is no possibility of acting on the mass of air loaded by the cylinders. Such systems will remain on the market for commercial reasons. In a cut–off operation, the hybrid engine model $\mathcal{M}_{4cyl}$ is fed by a decreasing sequence $q_a(k)$ of air intakes, which converge to the steady-state air quantity with pedal released, q_a^o. This results in an upper bound for the available torque. Hence, the cut-off problem is formulated as the optimization problem of maximizing the comfort, i.e. minimizing vehicle acceleration peaks, by a suitable control of fuel injection and spark advance. We identify as the starting point of the cut–off control horizon the time $t_0 = t_{k_0}$ at which $q_a(k_0) = q_a(k_0 - 1) = q_a(k_0 - 2) = q_a^o$, i.e. the time at which all the loaded cylinders' potential torques are at the steady–state value. To simplify the notation, we set $t_0 = 0$ and $k_0 = 0$.
To isolate oscillations from monotone behavior, consider the natural mode decomposition

$$\begin{bmatrix} x' \\ x \end{bmatrix} = \begin{bmatrix} P_1 \\ P_2 \end{bmatrix} \left(\zeta - (A^p)^{-1} b_0\right) = P\left(\zeta - (A^p)^{-1} b_0\right) \tag{4}$$

with $x' \in \mathbb{R}$, $x \in \mathbb{R}^2$, $P_1 \in \mathbb{R}^{1\times 3}$, and $P_2 \in \mathbb{R}^{2\times 3}$, where P is such that (1) is rewritten as follows

$$\begin{bmatrix} \dot{x}' \\ \dot{x} \end{bmatrix} = \begin{bmatrix} \lambda_1 & 0 \\ 0 & A \end{bmatrix} \begin{bmatrix} x' \\ x \end{bmatrix} + \begin{bmatrix} b' \\ b \end{bmatrix} u \;, \qquad \text{where } A = \begin{bmatrix} \lambda & -\mu \\ \mu & \lambda \end{bmatrix} \;. \tag{5}$$

Let $P^{-1} = [\hat{P}_1, \hat{P}_2]$, with $\hat{P}_1 \in \mathbb{R}^{3\times 1}$, $\hat{P}_2 \in \mathbb{R}^{3\times 2}$, (3) gives $a = c^p (A^p)^{-1} b_0 + c^p \hat{P}_1 x' + c^p \hat{P}_2 x$. Introducing $c = c^p \hat{P}_2 \in \mathbb{R}^{1\times 2}$, the oscillatory acceleration can be expressed as a linear function of the reduced state x, i.e.

$$\dot{x} = Ax + bu \;, \tag{6}$$
$$\tilde{a} = cx \;. \tag{7}$$

The objective of the cut–off control is to minimize the peaks of the acceleration $\tilde{a}(t)$ until they are less than a threshold of acceleration perception $\tilde{a}_{th} > 0$. The threshold condition $|\tilde{a}(t)| = |cx(t)| \leq \tilde{a}_{th}$ defines an unbounded stream $\mathcal{F}$ in the x sub–space. However, $\mathcal{F}$ is not a controlled invariant of the system, that is there exits initial conditions $x_0 \in \mathcal{F}$ for which no feasible torque u achieves $x(t) \in \mathcal{F}$ for all $t > 0$. Let $\|\cdot\|$ denote the Euclidean norm. Consider the circle

$$B_{\hat{\rho}} \;=\; \left\{ x \in \mathbb{R}^2 : \|x\| \leq \hat{\rho}, \quad \hat{\rho} = \tilde{a}_{th} \|c^T\|^{-1} \right\} \;. \tag{8}$$

In the free evolution of (5), the norm of $x(t)$ decreases over time, since $\frac{d(x^T x)}{dt} = 2\lambda\, x^T x$ and $\lambda < 0$. Therefore, if at some time $\bar{t}$, state x has been driven to the boundary $\partial B_{\hat{\rho}}$ of $B_{\hat{\rho}}$, i.e. $x(\bar{t}) \in \partial B_{\hat{\rho}}$, applying $u(t) = 0$ the trajectory remains in $B_{\hat{\rho}}$ and $|\tilde{a}(t)| < \tilde{a}_{th}$ for all $t \geq \bar{t}$. Cut–off control can be formulated as the optimization problem of steering the state x to the circle $B_{\hat{\rho}}$ minimizing the acceleration peaks. Once in $B_{\hat{\rho}}$, fuel injection can be shut off with vehicle oscillations below threshold. The cut–off optimization problem can then be formulated as follows.

Problem 1 *Given the engine hybrid model $\mathcal{M}_{4cyl}$, find $\hat{\mathbf{j}} \in \mathcal{J}_{4cyl}$ and $\hat{\mathbf{r}} \in \mathcal{R}_{4cyl}$ such that, for any initial state ζ_0 such that $x(0) = P_2\zeta_0 \notin B_{\hat{\rho}}$,*

$$\left. \sup_{0\leq t\leq T} |\tilde{a}(t)| \right|_{\substack{\mathbf{j} = \hat{\mathbf{j}} \\ \mathbf{r} = \hat{\mathbf{r}}}} \;=\; \min_{\substack{\mathbf{j} \in \mathcal{J}_{4cyl} \\ \mathbf{r} \in \mathcal{R}_{4cyl}}} \; \sup_{0\leq t\leq T} |\tilde{a}(t)|$$

$$
\text{subject to:}\begin{cases}
\text{Dynamics of Hybrid Model } \mathcal{M}_{4cyl} \text{ with} \\
q(k) = q_a^o, \quad \text{for all } k \geq 0, \\
\textit{FSM initial state: } \mathcal{S}_1 = H, \mathcal{S}_2 = I, \mathcal{S}_3 = C, \mathcal{S}_4 = E, \\
z_1(0) = 0, \ z_2(0) = z_3(0) = z_4(0) = Gq_a^o, \\
\zeta(0) = \zeta_0, \\
\phi_c(0) = 0, \\
x(T) = P_2\zeta(T) \in \partial B_{\hat{\rho}}
\end{cases}
$$

where $\tilde{a}(\cdot)$ is as in (7), $B_{\hat{\rho}}$ is as in (8) and the final time $T < \infty$ is unspecified.

Remark 2 *In Problem 1, the final time is not fixed but is determined by the control law that achieves the optimal value of the cost function.*

Note that, the above choice for the FSM initial state does not represent a limitation since any other admissible initial state can be obtained by a reordering of the cylinders.

3 Continuous-time model solution

The main difficulties in Problem 1 are that the plant to be controlled is hybrid and that the input signals **j** and **r** are bounded. Our strategy is to relax first the hybrid problem into the continuous time domain, maintaining the bound on the value the torque signal u can take, and then to map the solution back to the hybrid domain. The relaxed problem is formulated as follows:

Problem 3 *Given*

$$
\mathcal{U} = \{u : [0, +\infty) \to \mathrm{I\!R} \mid u(t) \textit{ measurable and } 0 \leq u(t) \leq M, \forall t \geq 0\} \quad (9)
$$

with $M = Gq_a^o$, find $\hat{u} \in \mathcal{U}$ such that, for any initial state $x_0 \notin B_{\hat{\rho}}$,

$$
\sup_{0 \leq t \leq T} |\tilde{a}(t)| \Big|_{u=\hat{u}} = \min_{u \in \mathcal{U}} \sup_{0 \leq t \leq T} |\tilde{a}(t)|
$$

$$
\text{subject to:}\begin{cases}
\dot{x}(t) = Ax(t) + bu(t) \\
x(0) = x_0 \\
x(T) \in \partial B_{\hat{\rho}}
\end{cases}
$$

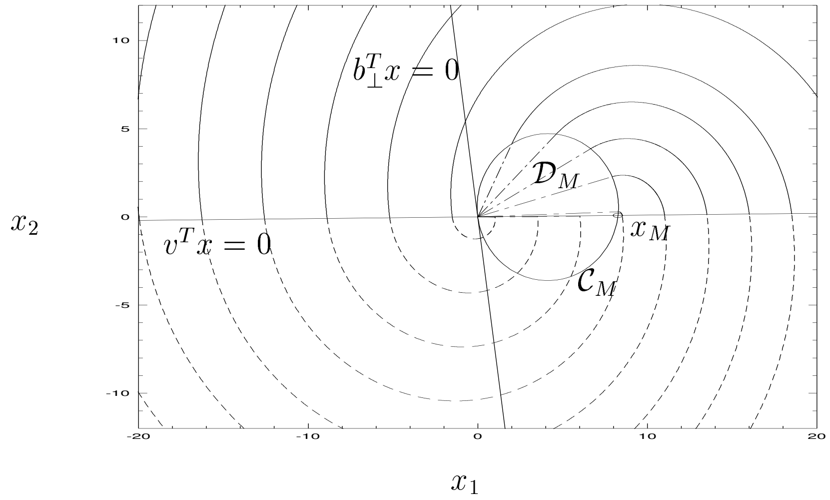

Fig. 2. Optimal trajectories for the relaxed problem. If $x \notin \mathcal{D}_M$, u is equal to either M (solid line) or 0 (dashed line). Otherwise $0 < u < M$ (dash-dot line).

where $\tilde{a}(\cdot)$ is as in (7), $B_{\hat{\rho}}$ is as in (8) and the final time $T < \infty$ is unspecified.

Note that, for some initial conditions a solution to Problem 3 may not exist or, if it does exist, may not be unique since the functional is not affected by the evolution after the time at which the acceleration maximum peak takes place. In the sequel existence is discussed and a solution is given. Let $R(\theta) \in \mathbb{R}^2$ be the counterclockwise rotation matrix of θ radians in $\mathbb{R}^2$ and, for any $z \in \mathbb{R}^2$, let $z_\perp$ denote $R(\frac{\pi}{2})z$. Let $x_M = -A^{-1}bM$ be the equilibrium point of (6) with $u = M$ and let $v = -\overrightarrow{vers}\,(x_M)_\perp$, where $\overrightarrow{vers}\,(x) \triangleq \frac{x}{\|x\|}$. In our previous paper [1], it was shown that there exists $u \in \mathcal{U}$, which steers the initial state x_0 of (6) to the origin along a straight line, provided that x_0 is inside the domain $\mathcal{D}_M = \mathcal{C}_M / \mathcal{A}_v$, where $\mathcal{A}_v = \left\{x \in \mathbb{R}^2 \mid (v^T x)(b^T R(-\frac{\pi}{2})x) > 0\right\}$ and $\mathcal{C}_M$ is the ball[5] given by $\left\{x \in \mathbb{R}^2 \mid \; x^T R(-\frac{\pi}{2})(Ax + bM) \leq 0\right\}$ (See Figure 2). Along these trajectories, the cost function $|\tilde{a}(\cdot)|$ monotonically decreases to zero. However, with this control law, the time to reach $B_{\hat{\rho}}$ becomes unbounded as x_0 approaches the line $v^T x = 0$. In this paper, we propose a modified control law that eliminates this problem by giving up (slightly) optimality for particular trajectories. However, optimality can be approached infinitely close by our control strategy as shown in the following theorem.

Theorem 4 *Consider an initial state $x_0 \notin B_{\hat{\rho}}$. Let $\mathcal{U}' \subset \mathcal{U}$ be the class of all input signals $u' \in \mathcal{U}$ which steer the state x of system (6) from x_0 to a point on $\partial B_{\hat{\rho}}$. Let $\psi(u', x_0, t)$, with $t \in [0, T]$, denote the trajectory from x_0 to $x_T = \psi(u', x_0, T) \in \partial B_{\hat{\rho}}$ corresponding to some $u' \in \mathcal{U}'$, where T depends on*

[5] $\mathcal{C}_M$ has center in $\frac{M}{2\mu}R(\frac{\pi}{2})b$ and radius $\frac{M}{2\mu}\|b\|$. Its boundary contains the origin (where its tangent is collinear to vector b) and the equilibrium point x_M.

u' and x_0. Let

$$\tilde{A}(x_0) = \inf_{u' \in \mathcal{U}'} \sup_{0 \le t \le T} |c\psi(u', x_0, t)| = \inf_{u' \in \mathcal{U}'} \sup_{0 \le t \le T} |\tilde{a}(t)| \Big|_{u=u'} .$$

For any $x \notin B_{\hat{\rho}}$, consider the feedback control

$$\hat{u} = \begin{cases} \begin{cases} 0 & \text{if } v^T x \ge 0 \\ M & \text{if } v^T x < 0 \end{cases} & \text{if } x \notin \mathcal{D}_M \\ \\ \begin{cases} -\frac{x^T R(-\frac{\pi}{2}) A x}{x^T R(-\frac{\pi}{2}) b} & \text{if } (R(\theta)v)^T x \le 0 \\ 0 & \text{if } (R(\theta)v)^T x > 0 \end{cases} & \text{if } x \in \mathcal{D}_M \end{cases} . \tag{10}$$

If $\|x_M\| \ge \hat{\rho}$ then

A1. *if $(cx_M)(cb) > 0$ control (10) with θ set to any value in the open interval $(0, \sin^{-1}(\eta))$, where $\eta = \frac{-\lambda}{\sqrt{\lambda^2+\mu^2}}$ denotes the damping ratio of system (5), steers in finite time the initial state $x_0 \notin B_{\hat{\rho}}$ to $\partial B_{\hat{\rho}}$ and is optimal for Problem 3, i.e. $\tilde{A}(x_0) = \sup_{0 \le t \le T} |\tilde{a}(t)| \Big|_{u=\hat{u}}$.*

A2. *if $(cx_M)(cb) \le 0$ there is a set of initial conditions $\mathcal{X}_0 \subset \mathbb{R}^2 / B_{\hat{\rho}}$ such that for any $x_0 \in \mathcal{X}_0$ no optimal solution in finite time exists. However, for any $\epsilon > 0$ there exists $\theta > 0$ such that control (10) steers any $x_0 \notin B_{\hat{\rho}}$ to $\partial B_{\hat{\rho}}$ in finite time, with $\sup_{0 \le t \le T} |\tilde{a}(t)| \Big|_{u=\hat{u}} - \tilde{A}(x_0) < \epsilon$ if $x_0 \in \mathcal{X}_0$, and with $\sup_{0 \le t \le T} |\tilde{a}(t)| \Big|_{u=\hat{u}} = \tilde{A}(x_0)$ if $x_0 \notin \mathcal{X}_0$.*

else, if $\|x_M\| < \hat{\rho}$,

B. *control (10) with $\theta = 0$, is optimal for Problem 3.*

It is interesting to note that for all models of existing cars available to us, $(cx_M)(cb) > 0$ and, hence, (10) was actually optimal. Figure 2 shows the closed loop phase space under control (10) with $(cx_M)(cb) > 0$ and $\theta \simeq 0$. Observing that the greater is M the lower are the acceleration peaks, we can make use or air flow regulation available for idle control to set q_a^o it its maximum value.

The proof of Theorem 4, (see [2],[3]) is based on the analysis of the reachable sets for system (6) with control $u \in \mathcal{U}$.

Lemma 5 *(See [3]) For any $x_0 \in \mathbb{R}^2$, the closed loop trajectory $\psi(u, x_0, t)$ of* *system (6) under control*

$$u = \begin{cases} \hat{u}(x) & \text{if } x \notin B_{\hat{\rho}} \\ 0 & \text{if } x \in B_{\hat{\rho}} \end{cases} \tag{11}$$

with $\hat{u}(x)$ as in (10), is such that $\|x(t)\| = \|\psi(u, x_0, t)\|$ strictly decreases over time and converges to the origin.

Trajectories of (6) under control (10) are characterized by the following results.

Proposition 6 *(See [3]) Let $h = \overrightarrow{vers}\left((cA)^T\right)$ and $\psi(\hat{u}, x_0, t)$ be the solution of (6), from x_0, with $\hat{u}$ as in (10).*
(1) *If $\tau > 0$ is a point of local maximum for $|\tilde{a}(t)|$ and $\hat{u}(t)$ is continuous at $t = \tau$ and constant in a neighborhood of $t = \tau$, then $\hat{u}(\tau) \in \{0, M\}$ and $x_\tau = \psi(\hat{u}, x_0, \tau)$ is such that*

$$h^T \left(x_\tau - x_M \frac{\hat{u}(\tau)}{M} \right) = 0 \ . \tag{12}$$

(2) *If $\tau_1, \tau_2 > 0$ are two successive local maxima for $|\tilde{a}(t)|$, then $\tau_2 - \tau_1 \leq \pi/\mu$ (where equality holds if $\hat{u}(t)$ is continuous at both τ_1 and τ_2), and $|\tilde{a}(\tau_1)| > |\tilde{a}(\tau_2)|$.*

4 Hybrid system control scheme

Control law (10) is clearly not feasible for the hybrid model $\mathcal{M}_{4cyl}$, introduced in Section 2, since, for the continuous case, there is no limitation on the torque other than it must be bounded to $[0, M]$. Hence, the acceleration peak achieved by the control law in the relaxed domain is a lower bound for the hybrid problem. Our strategy is to "approximate" the previous control law to take into account the additional limitations on the input signals so that the performance of the approximated control law is provably "close" to the optimal one for the relaxed problem.

There are three constraints that, so far, have not been taken into account, namely:

(a) *the available torque is limited to* 0 *and to the interval* $[r_{\min}M, M]$; in the relaxed control problem it was assumed instead that the torque could take values in the closed interval $[0, M]$. Since the optimal control law determined in the previous section, was bang-bang everywhere except for a (small) region, our solution is to over–constrain the optimization problem limiting our attention to bang–bang torque that can take the two extreme values 0 and M only. This corresponds to setting the spark advance inputs $r_i = 1$ everywhere, and to using as control only the variables j_i. We will show that restricting our attention to bang-bang controls does not affect substantially the quality of the solution and does simplify the optimization problem at hand.

(b) *There is a delay between the time of injection and the time at which the corresponding torque is generated.* Hence, when the decision on the injection signal is taken, we need to "predict" the value that the state variables will assume at the time the torque is generated. For the sake of notational simplicity, set $x(k) \triangleq x(t_k)$ for all k. The control signal $j_i(k)$, at the current time t_k (corresponding to an $E \rightarrow H$ transition of the $i-$th cylinder), produces, at the next expansion run of the $i-$th cylinder, the torque $u(k+3)$. This torque is applied to the continuous system during the interval $[t_{k+3}, t_{k+4})$, steering the state from $x(k+3)$ to $x(k+4)$. A prediction of $\tilde{x}_3(k)$ is obtained from $x(k)$ by a forward integration of (6).

(c) *The control signal has to be synchronized with powertrain dynamics.* Hence, in general, the generated torque cannot switch *exactly* on a given switching line. This issue is the main difficulty for devising the control strategy for the hybrid system, and is the main subject of this section.

In the following we propose a control strategy in terms of the injection signals j_i for the hybrid model $\mathcal{M}_{4cyl}$. An implementation requirement is that the control algorithm be run at the top dead center instants t_k, deciding the injection signal based only on the information available at t_k, i.e. only on the knowledge of state samples $x(k) = x(t_k)$.

4.1 The hybrid switching line

The injection control is defined according to a switching curve $\sigma(x) = 0$, where $\sigma : \mathbb{R}^2 \rightarrow \mathbb{R}$. Due to the synchronization problem mentioned in point (c) above, $\sigma(x) = 0$ defines an ideal switching location for the torque signal $u(t)$. If it is predicted that $x(t)$ will cross the switching line at some $t \in (t_{k+3}, t_{k+4})$, we could toggle j_i either at t_k or t_{k+1}. The difference $t_{k+1} - t_k$ depends on the crankshaft revolution speed $\omega_c(t)$. Given $\sigma(x)$, the control law is choosen as:

$$\hat{j}_i(k) = \begin{cases} 0 & \text{if } \tilde{x}_3(k) \in B_{\hat{\rho}} \\ \begin{cases} 0 \text{ if } \sigma(\tilde{x}_3(k)) \geq 0 \\ 1 \text{ if } \sigma(\tilde{x}_3(k)) < 0 \end{cases} & \text{if } \tilde{x}_3(k) \notin B_{\hat{\rho}} \ . \end{cases} \tag{13}$$

In the sequel we assume that the prediction $\tilde{x}_3(k)$ is correct, i.e. $\tilde{x}_3(k) = x(k+3)$. The simplest approximation to the continuous control law for the hybrid case, is to use the switching line

$$\sigma(x) = v^T x. \tag{14}$$

Once the bang–bang control law is selected, we need to prove its convergence and performance. Convergence is not obvious; in fact, recall that, even in the continuous case, we had to finess the control law inside $\mathcal{D}_M$ to guarantee finite time convergence to $B_{\hat{\rho}}$.

The properties of (13) depend on the position of x_M with respect to $B_{\hat{\rho}}$. If $\|x_M\| \leq \hat{\rho}$, control law (13), with $\sigma(x)$ as in (14), will be proven to yield trajectories that converge to $B_{\hat{\rho}}$ if the engine speed is larger than an appropriate bound. If $\|x_M\| > \hat{\rho}$, we will show that this control law may not converge and $\sigma(x)$ needs to be modified to guarantee convergence.

4.2 Convergence Analysis

The continuous torque feedback (10) caused a monotonic decrease in the norm of x with time, see Lemma 5. We cannot always claim the same behavior for the hybrid control mainly due to the effects of the discretization of the decision points. Since, as observed in Section 3, $\|x(t)\|$ monotonically converges to zero when torque $u = 0$ is applied, we need to worry only when the generated torque under feedback (13), continues to be $u = M$, while the continuous torque feedback (10) calls for $u = 0$. Indeed, due to this delay, the closed loop hybrid system may not exhibit a monotonic decrease in the norm of x with time. The set of points such that a control $u = M$ applied for time Δ causes an increase in norm is

$$\mathcal{N}'_\Delta = \{x \in \mathbb{R}^2 \mid \|x\| < \|e^{A\Delta}(x - x_M) + x_M\|\}. \tag{15}$$

Note that

- $x_M \in \partial \mathcal{N}'_\Delta$ for all $\Delta > 0$;
- $\lim_{\Delta \to 0} \mathcal{N}'_\Delta = \mathcal{N}_0$ where $\mathcal{N}_0$ is the disk $\left\{x \mid x^T A(x - x_M) \geq 0\right\}$, with center $-\frac{M}{2\lambda}b$ and boundary containing both the origin and x_M;
- $\mathcal{N}'_\Delta|_{\Delta=0} = \emptyset$.

Since $\lim_{\Delta\to 0}\mathcal{N}'_\Delta \neq \mathcal{N}'_\Delta|_{\Delta=0}$, extend $\mathcal{N}'_\Delta$ by continuity as follows

$$\mathcal{N}_\Delta = \begin{cases} \mathcal{N}'_\Delta & \text{if } \Delta > 0, \\ \mathcal{N}_0 & \text{if } \Delta = 0. \end{cases} \tag{16}$$

The relative position of $\mathcal{N}_\Delta$ and $B_{\hat\rho}$ is important to determine the convergence of the closed loop system. This position depends on the location of x_M with respect to $B_{\hat\rho}$. We divide the convergence analysis in two parts, namely, $\|x_M\| \leq \hat\rho$ and $\|x_M\| > \hat\rho$. The first case is of theoretical interest only since, for all model parameters seen in commercial cars, the second case applies.

Let $\varphi(\hat{j}_i, x_0, t)$ denote a generic trajectory in the reduced state space x of the continuous–time dynamics of the hybrid model $\mathcal{M}_{4cyl}$ obtained under control $\hat{j}_i(k)$ as in (13) with $x(0) = x_0$. Define the sequence $\Delta_k \triangleq t_{k+1} - t_k$ of intervals between transitions in the FSMs.

Remark 7 *If $\Delta_k = \frac{\pi}{\mu}$ the generated torque u under control (13) switches to 0 when it should switch to M and vice versa. The resulting control performs poorly. For this reason we restrict engine speed to $\omega_c(t) > 2\mu$ for all $t > 0$, and hence $\Delta_k < \frac{\pi}{2\mu}$ for all $k > 0$.*

4.3 Convergence for the case $\|x_M\| \leq \hat\rho$

Lemma 8 *Let $\|x_M\| \leq \hat\rho$. Let $\mathcal{T}$ be the set of points x where injection as in (13) is set to zero, i.e. $\mathcal{T} = B_{\hat\rho} \cup \{x \in \mathbb{R}^2 | \sigma(x) \geq 0\}$. There exists $\Delta_\mathcal{N} > 0$ such that for all $\Delta \in [0, \Delta_\mathcal{N})$,*

$$\mathcal{N}_\Delta \subset \mathcal{T}. \tag{17}$$

PROOF. By definition (16), $x_M \in \partial\mathcal{N}_\Delta$ for all Δ. By hypothesis, we have also $x_M \in B_{\hat\rho}$. Both the origin and x_M belong to $\partial\mathcal{N}_0$. Hence, the line $v^T x = 0$ intersects $\mathcal{N}_0$. By construction, $v^T b > 0$ so the centre of $\mathcal{N}_0$ belongs to the half plane $v^T x \geq 0$. As a consequence, $\mathcal{N}_0 \setminus \{x \in \mathbb{R}^2 | v^T x \geq 0\} \subset B_{\hat\rho}$ and (17) holds for $\Delta = 0$. By continuity, there exists a right neighborhood I of $\Delta = 0$ for which the same result holds. Set $\Delta_\mathcal{N} = \sup\ I$. Q.E.D.

Note that the interval for which $\mathcal{N}_\Delta \subset \mathcal{T}$ holds may be unbounded if $\|x_M\| \ll \hat\rho$.

Proposition 9 *Let $\|x_M\| \leq \hat\rho$. Consider all trajectories $\varphi(\hat{j}_i, x_0, t)$ under control $\hat{j}_i(k)$ as in (13) with $\sigma(x)$ defined as in (14). There exists engine speed*

$\omega_{\min} = \frac{\pi}{\Delta_{\max}}$ *such that, if* $\omega_c(t) > \omega_{\min}$ *for all* t*, for all initial conditions* x_0 *trajectories* $\varphi(\hat{j}_i, x_0, t)$ *converge to* $B_{\hat{\rho}}$*.*

PROOF. By Lemma 8, for all $\Delta \in [0, \Delta_{\mathcal{N}}), \mathcal{N}_\Delta \subset \mathcal{T}$. According to Remark 7, set $\Delta_{\max} = \min\{\frac{\pi}{2\mu}, \Delta_{\mathcal{N}}\}$. For any trajectory with $\omega_c(t) > \frac{\pi}{\Delta_{\max}}$ for all $t > 0$, necessarily $\|x(k+1)\| < \|x(k)\|$ for all $k > 0$ and convergence to $B_{\hat{\rho}}$ is ensured. Q.E.D.

The derived bound $\Delta_{\max}$ may not be tight (especially when $\|x_M\|$ approaches $\hat{\rho}$). A tighter upper bound can be obtained modifying properly the algorithm illustrated in Section 4.4, which does not require condition (17).

4.4 Convergence for the case $\|x_M\| > \hat{\rho}$

Let us examine the behavior of trajectories when intersecting $v^T x = 0$ between $B_{\hat{\rho}}$ and x_M. As illustrated in the continuous control section, points $x_e(\bar{u}) = -A^{-1}b\bar{u}$ are equilibrium points for control $u = \bar{u}$. For all $\bar{u} \in (0, M)$ points $x_e(\bar{u})$ belong to the segment from the origin to x_M. Moreover, $v^T\psi(M, x_e(\bar{u}), t) > 0$ for all $t \in (0, \bar{t}]$ and $v^T\psi(0, x_e(\bar{u}), t) < 0$ for all $t \in (0, \bar{t}]$, with some $\bar{t} > 0$. This motion may cause the control law to switch across $v^T x = 0$ indefinitely, without ever reaching $B_{\hat{\rho}}$. This behavior is analogous to the infinitely slow motion encountered in Section 3. There we introduced a small but finite sector forcing $u = 0$ in the proximity of the segment. Hence, we must make sure never to apply $u = M$ in the region shaded in Figure 3. To define a switching line that satisfies this requirement, we make use of the intersections between $\mathcal{N}_\Delta$ and $B_{\hat{\rho}}$. The existence of these intersections is analyzed in the following Lemma.

Lemma 10 *Let* $\|x_M\| > \hat{\rho}$*. There exists* $\Delta_{\mathcal{N}} > 0$ *such that for all* $\Delta \in [0, \Delta_{\mathcal{N}})$*,*

$$\partial\mathcal{N}_\Delta \cap \partial B_{\hat{\rho}} = \{x_c^{(1)}, x_c^{(2)}\} \text{ with } x_c^{(1)} \neq x_c^{(2)}. \tag{18}$$

PROOF. Since $O \in \partial\mathcal{N}_0$, $x_M \in \partial\mathcal{N}_0$ and $x_M \notin B_{\hat{\rho}}$, condition (18) holds for $\Delta = 0$. By continuity, there exists a right neighborhood I of $\Delta = 0$ in which the same result holds. Set $\Delta_{\mathcal{N}} = \sup\ I$. Q.E.D.

For all Δ' such that $\partial B_{\hat{\rho}} \cap \partial\mathcal{N}_{\Delta'} = \emptyset$, $B_{\hat{\rho}} \subset \mathcal{N}_{\Delta'}$. Thus trajectories with $\omega_c(t) \leq \frac{\pi}{\Delta'}$ for some t, may "jump" $B_{\hat{\rho}}$ under $u(k) = M$. If $B_{\hat{\rho}}$ is made larger,

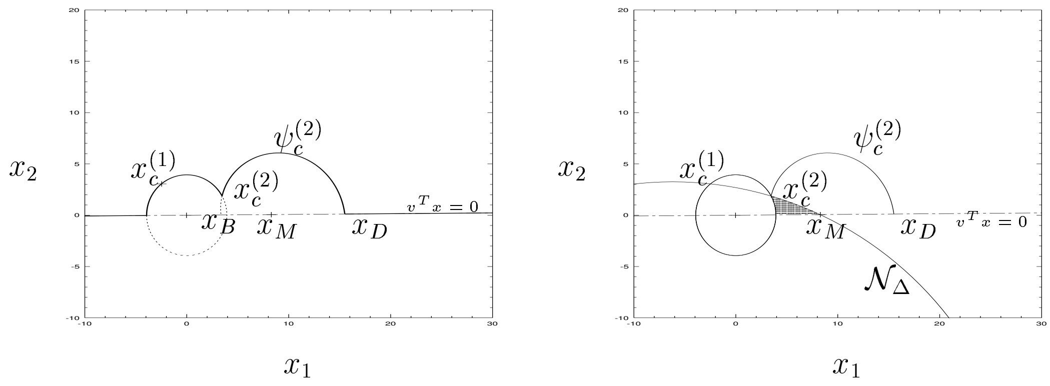

Fig. 3. Hybrid switching line for $\|x_M\| > \rho$ and convergence analysis "close" to B_ρ.

than this problem disappear. However, increasing the acceleration threshold decreases driving comfort. Let

$$\Delta_{\mathcal{N}}^0 = \min\{\frac{\pi}{2\mu}, \Delta_{\mathcal{N}}\}, \tag{19}$$

where $\Delta_{\mathcal{N}}$ is as in Lemma 10 and bound $\frac{\pi}{2\mu}$ comes from Remark 7. In the sequel we consider only trajectories such that $\omega_c(t) > \frac{\pi}{\Delta}$ for all $t > 0$, for some $\Delta < \Delta_{\mathcal{N}}^0$ so that $\partial B_{\hat{\rho}} \cap \partial \mathcal{N}_\Delta \neq \emptyset$.

Consider point $x_c^{(2)}$ as in (18) and let x_B denote the first intersection point of the trajectory $\psi(M, x_c^{(2)}, t)$ with the line $v^T x = 0$. Let $\psi_{M^-}(x, \alpha) = e^{-A\frac{\alpha}{\mu}}(x - x_M) + x_M$ denote the point such that $\psi(M, \psi_{M^-}(x, \alpha), \frac{\alpha}{\mu}) = x$. Introduce the arc $\psi_c^{(2)} = \left\{x \in \mathbb{R}^2 | x = \psi_{M^-}(x_B, \alpha) \text{ with } \alpha \in [0, \pi]\right\}$ obtained by back integration with $u = M$ from x_B to

$$x_D = \psi_c^{(2)}(\pi), \tag{20}$$

with $v^T x_D = 0$. By construction, $x_c^{(2)} \in \psi_c^{(2)}$.

The switching function is modified to include the arc $\psi_c^{(2)}$:

$$\sigma(x) = \begin{cases} (v^T b/\|b\|)^{-1} v^T x, & \text{if } (b_\perp{}^T x \leq b_\perp{}^T x_B) \ \vee \ (b_\perp{}^T x \geq b_\perp{}^T x_D) \\ \\ (b/\|b\|)^T (x - x_b), & \text{if } b_\perp{}^T x_B < b_\perp{}^T x < b_\perp{}^T x_D \\ \text{with } x_b \text{ s.t. } (b_\perp{}^T (x - x_b) = 0) \ \wedge (\ x_b \in \psi_c^{(2)}) & \end{cases} \tag{21}$$

Because of the presence of $\psi_c^{(2)}$, $\sigma(x)$ depends on Δ.

Proposition 11 *Let $\|x_M\| > \hat{\rho}$. Consider all trajectories $\varphi(\hat{j}_i, x_0, t)$ under*

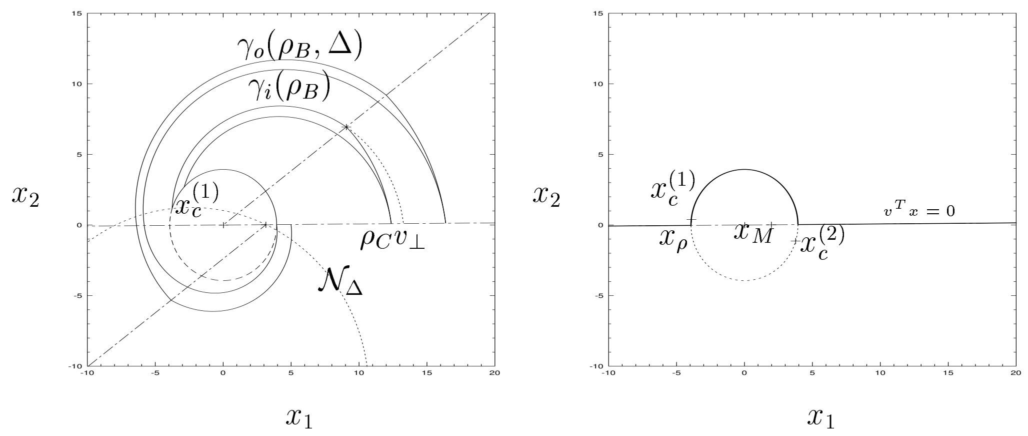

Fig. 4. Switching surface for $\|x_M\| \leq \rho$ and convergence analysis from $x^1_{e^+} = \rho_C v_\perp$.

control $\hat{j}_i(k)$ as in (13) with $\sigma(x)$ defined as in (21), with engine speed $\omega_c(t) > \frac{\pi}{\Delta^0_{\mathcal{N}}}$ $\forall t \geq 0$, where $\Delta^0_{\mathcal{N}}$ is as in (19). There exists engine speed $\omega_{\min} = \frac{\pi}{\Delta_{\max}}$ such that, if $\omega_c(t) > \omega_{\min}$ for all t, for all initial conditions x_0 trajectories $\varphi(\hat{j}_i, x_0, t)$ converge to $B_{\hat{\rho}}$ in finite time.

PROOF. Let $e^+ = \{x \in \mathbb{R} | v^T x = 0 \wedge v_\perp^T x > 0\}$ and $e^- = \{x \in \mathbb{R} | v^T x = 0 \wedge v_\perp^T x < 0\}$, be the two half lines that define the switching line. To prove convergence we will examine the intersections of the trajectories on e^+. In particular, there are three critical points on e^+ that determine the behavior of the trajectories:

(1) $\hat{\rho} v_\perp$, the intersection of e^+ with $\partial B_{\hat{\rho}}$,

(2) $\rho_C v_\perp$, where $\rho_C v_\perp$ is defined as follows: consider the crossing point $x^1_{e^+} = \rho v_\perp$ with $\rho > \hat{\rho}$. Introduce the curve $\gamma_o(\rho, \Delta)$, which represents the trajectory from $x^1_{e^+} = \rho v_\perp$ in the x sub-space obtained with switchings of the torque signal occurring with the longest delay Δ with respect to the instant of intersection with the line $v^T x = 0$. Let $\angle(v_1, v_2) \triangleq \cos^{-1} \frac{v_1^T v_2}{\|v_1\| \, \|v_2\|}$ denote the unsigned angle between two vectors v_1 and v_2. Curve $\gamma_o(\rho, \Delta)$ consists of the following arcs of bang-bang trajectories:
   - $\psi(0, x^1_{e^+}, t)$ with $t \in [0, \Delta]$, from $x^1_{e^+}$ to $x^\Delta_{e^+} = \psi(0, x^1_{e^+}, \Delta)$;
   - $\psi(M, x^\Delta_{e^+}, t)$ with $t \in [0, \frac{1}{\mu}\angle(x^\Delta_{e^+} - x_M, -v_\perp)]$, from $x^\Delta_{e^+}$ to $x^1_{e^-} = \psi(M, x^\Delta_{e^+}, \frac{1}{\mu}\angle(x^\Delta_{e^+} - x_M, -v_\perp))$;
   - $\psi(M, x^1_{e^-}, t)$ with $t \in [0, \Delta]$, from $x^1_{e^-}$ to $x^\Delta_{e^-} = \psi(M, x^1_{e^-}, \Delta)$;
   - $\psi(0, x^\Delta_{e^-}, t)$ with $t \in [0, \frac{1}{\mu}\angle(x^\Delta_{e^-}, -v_\perp)]$, from $x^\Delta_{e^-}$ to $x_{\gamma_o} = \psi(0, x^\Delta_{e^-}, \frac{1}{\mu}\angle(x^\Delta_{e^-}, -v_\perp))$.

   The end points of $\gamma_o(\rho, \Delta)$ are $x^1_{e^+}$ and x_{γ_o} both on line e^+. See Figure 4. Consider a value Δ, correspondingly define ρ_C such that $x_c^{(1)} \in \gamma_o(\rho_C, \Delta)$.

(3) $\rho_B v_\perp$ where $\rho_B = e^{-\lambda\frac{2\pi}{\mu}}\hat{\rho} + (1 + e^{-\frac{\lambda\pi}{\mu}})\|x_M\|$. $\rho_B v_\perp$ is the point on e^+ obtained by back integration of equations (6) starting from $\hat{\rho} v_\perp$ under

torque (10).

The main idea of the proof is to show that trajectories $\varphi(\hat{j}_i, x_0, t)$ starting from initial conditions x_0 that yield the first intersection $x^1_{e^+} = \rho v_\perp$ with e^+ at time $t^1_{e^+}$

Case 1: inside $B_{\hat\rho}$ will remain there;

Case 2: between $\hat\rho v_\perp$ and $\rho_C v_\perp$, will enter $B_{\hat\rho}$ in less than one revolution around O and set control to zero;

Case 3: between $\rho_C v_\perp$ and $\rho_B v_\perp$, will intersect in finite time e^+ in one of the other regions, after a finite number $n_C \geq 0$ of revolutions around the origin;

Case 4: beyond $\rho_B v_\perp$ will intersect in finite time e^+ in one of the other regions, after a finite number $n_B \geq 1$ of revolutions around the origin. By hypothesis $\omega_c(t) > \frac{\pi}{\Delta^0_{\mathcal{N}}} \geq 2\mu$, hence this intersection occurs with $u = 0$.

Case 1. Intersection point $x^1_{e^+} = \rho v_\perp$ with $\rho \leq \hat\rho$. Let $\bar{k}$ be such that $t_{\bar{k}+3} \leq t^1_{e^+} < t_{\bar{k}+4}$. The next decision point $x(\bar{k}+4) = \varphi(\hat{j}_i, x_0, t_{\bar{k}+4})$ has norm less than ρ. Since $x(\bar{k}+4)$ is inside $B_{\hat\rho}$, $\hat{j}_i(k) = 0$, $\forall k \geq \bar{k}$. Hence, $\varphi(\hat{j}_i, x_0, t)$ remain inside $B_{\hat\rho}$, for all $t \geq t^1_{e^+}$.

Case 2. Intersection point $x^1_{e^+} = \rho v_\perp$ with $\hat\rho < \rho < \rho_C$. For this part of the proof refer to Figure 5. Let $t_\sigma \geq t^1_{e^+}$ denote the lowest time such that $\sigma(\varphi(\hat{j}_i, x_0, t_\sigma)) = 0$, and let $\bar{k}$ be such that $t_{\bar{k}+3} \leq t_\sigma < t_{\bar{k}+4}$. For trajectories with $\omega_c(t) > \frac{\pi}{\Delta}$ for all $t > 0$, the next decision point $x(\bar{k}+4)$, at time $t_{\bar{k}+4} = t_{\bar{k}+3} + \Delta_{\bar{k}+3} \leq t_{\bar{k}+3} + \frac{\pi}{2\mu}$, belongs to the set $\mathcal{S}_\Delta$ defined as

$$\begin{aligned}\mathcal{S}_\Delta = &\Big\{x \in \mathbb{R}^2 | x = e^{A\tau}\psi_c^{(2)}(\alpha), \text{with } \ \alpha \in [0, \pi] \ \text{ and } \tau \in [0, \Delta]\Big\} \ \cup \\ &\Big\{x \in \mathbb{R}^2 | x = e^{A\tau}\rho_0 v_\perp, \text{with } \ \rho_0 \in [\|x_D\|, \rho_C] \ \text{ and } \tau \in [0, \Delta]\Big\}, \quad (22)\end{aligned}$$

where x_D is as in (20). If $x(\bar{k}+4) \in B_{\hat\rho}$, $\hat{j}_i(\bar{k}+1) = 0$ and $\varphi(\hat{j}_i, x_0, t) \in B_{\hat\rho}$ for all $t \geq t_{\bar{k}+4}$. If $x(\bar{k}+4) \notin B_{\hat\rho}$, $\hat{j}_i(\bar{k}+1) = 1$ and $u(\bar{k}+4) = M$. Note that the trajectories $\varphi(\hat{j}_i, x_0, t)$ coincide with $\psi(M, x(\bar{k}+4), t - t_{\bar{k}+4})$ for $t > t_{\bar{k}+4}$, until they either enter $B_{\hat\rho}$ or intersect e^-. If

$$\mathcal{S}_\Delta \cap \gamma_o(\rho_C, \Delta) = \emptyset \qquad (23)$$

$\varphi(\hat{j}_i, x_0, t)$ are bounded by $\gamma_o(\rho_C, \Delta)$ and $\psi_c^{(2)}$ and enter $B_{\hat\rho}$ at some time $t_{\hat\rho} \leq t_{\bar{k}+4} + \frac{\pi}{\mu} \leq t_{\bar{k}+3} + \frac{3\pi}{2\mu}$. Since $\gamma_o(\rho_C, \Delta)$ and $\psi_c^{(2)}$ intersect $\partial B_{\hat\rho}$ at $x_c^{(1)}$ and $x_c^{(2)}$ respectively, $\varphi(\hat{j}_i, x_0, t)$ enter $B_{\hat\rho}$ under $u(t) = M$ through the arc $\partial B_{\hat\rho} \setminus \mathcal{N}_\Delta$. Let $\bar{K} > \bar{k}+4$ be such that $t_{\bar{K}-1} \leq t_{\hat\rho} < t_{\bar{K}}$. Since $x(t_{\hat\rho}) \notin \mathcal{N}_\Delta$, $\psi(M, x(t_{\hat\rho}), t)$ is inside $B_{\hat\rho}$ for all $t \in [0, \Delta]$. Hence, $x(\bar{K}) \in B_{\hat\rho}$, the injection switches to zero and $\varphi(\hat{j}_i, x_0, t) \in B_{\hat\rho}$ for all $t \geq t_{\hat\rho}$.

Note that

$$\lim_{\Delta\to 0} \mathcal{S}_\Delta = \Sigma_0 \triangleq \left\{ x \in \mathbb{R}^2 \mid \sigma(x) = 0,\ \|x\| \geq \hat{\rho},\ 0 < v_\perp^T x < \rho_C \right\}, \quad (24)$$

$$\lim_{\Delta\to 0} \gamma_o(\rho_C, \Delta) = \psi_c^{(1)} \triangleq \left\{ x \in \mathbb{R}^2 \mid x = \psi_{M^-}(x_c^{(1)}, \alpha),\ \alpha \in [0, \alpha_c^{(1)}] \right\}, \quad (25)$$

where $\alpha_c^{(1)} = \angle((x_c^{(1)} - x_M), v_\perp)$. Since $x_c^{(1)} \neq x_c^{(2)}$, $\psi_c^{(1)} \cap \Sigma_0 = \emptyset$ and (23) holds for $\Delta = 0$. By continuity there exists a right neighborhood I of $\Delta = 0$ in which the same result holds. Set $\Delta'_D = \sup\ I$. To find Δ'_D, we compute the zero of a function $f(\Delta)$ which is positive if (23) holds, negative otherwise. To define $f(\Delta)$, determine the trajectory $\psi_c^{(\Delta)}$, where $\psi_c^{(\Delta)}(\alpha) = \psi_{M^-}(\bar{x}_\Delta, \alpha)$, with $\alpha \in [0, \pi]$, and $v^T \bar{x}_\Delta = 0$ such that $\psi_c^{(\Delta)}$ is tangent to $\psi_{c\Delta}^{(2)}(\cdot) \triangleq e^{A\Delta}\psi_c^{(2)}(\cdot)$ at point $x_\Delta = \psi_{c\Delta}^{(2)}(\alpha_\Delta)$. At point x_Δ

$$-\left.\frac{\partial \psi_{c\Delta}^{(2)}(\alpha)}{\partial \alpha}\right|_{\alpha=\alpha_\Delta} // A\left(\psi_{c\Delta}^{(2)}(\alpha_\Delta) - x_M\right). \quad (26)$$

Condition (26) is satisfied for $\alpha_\Delta = \mu\Delta + \angle\left(-v_\perp, (e^{A\Delta}x_M - x_M)\right)$. Consider $x_\Delta^{(1)} = \psi_{M^-}(x_A, \alpha_\Delta^{(1)})$, with $\alpha_\Delta^{(1)} = \angle(-v_\perp, x_\Delta)$, and define

$$f(\Delta) = \|x_\Delta^{(1)} - x_M\| - \|x_\Delta - x_M\|. \quad (27)$$

Hence Δ'_D is the unique root of $f(\Delta)$ in $(0, \Delta_\mathcal{N}]$. Let

$$\Delta_D = \min\left\{\Delta'_D, \Delta^0_\mathcal{N}\right\}. \quad (28)$$

Consider all possible trajectories $\varphi(\hat{j}_i, x_0, t)$ starting from $x^1_{e^+} = \rho v_\perp \in e^+$ with $\rho \in (\hat{\rho}, \rho_C)$ and with

$$\omega_c(t) > \frac{\pi}{\Delta_D} \text{ for all } t > 0. \quad (29)$$

Within one revolution around the origin, they have a decision point inside $B_{\hat{\rho}}$ and switch control to zero.

Case 3. Intersection point $x^1_{e^+} = \rho v_\perp$ with $\rho_C \leq \rho < \rho_B$. Let $\gamma_i(\rho)$ denote the curve composed of the two arcs of trajectory

- $\psi(M, x^1_{e^+}, t)$ with $t \in [0, \frac{\pi}{\mu}]$, from $x^1_{e^+} = \rho v_\perp$ to $x^i_{e^-} = \psi(M, x^1_{e^+}, \frac{\pi}{\mu})$;
- $\psi(0, x^i_{e^-}, t)$ with $t \in [0, \frac{\pi}{\mu}]$, from $x^i_{e^-}$ to $x_{\gamma_i} = \psi(0, x^i_{e^-}, \frac{\pi}{\mu})$.

The end points of $\gamma_i(\rho)$ are $x^1_{e^+}$ and x_{γ_i}, both on e^+. Consider a generic trajectory $\varphi(\hat{j}_i, x_0, t)$ crossing e^+ at $x^1_{e^+}$ at time $t^1_{e^+}$, let $t^2_{e^+} \geq t^1_{e^+}$ denote the time at which it intersects a second time the half line e^+ at some point $x^2_{e^+}$. All possible $\varphi(\hat{j}_i, x_0, t)$ crossing x_{e^+}, are contained for $t \in [t^1_{e^+}, t^2_{e^+}]$ in the set delimited by $\gamma_o(\rho, \Delta)$ and $\gamma_i(\rho)$, and the segment from x_{γ_o} to x_{γ_i}, as shown in Figure 4. Time $t^2_{e^+} - t^1_{e^+}$ is bounded above by $\frac{2\pi}{\mu}$.

We want to guarantee that $\rho_C \geq \|x_D\|$, with x_D as in (20), so that both curves $\gamma_i(\rho_C)$ and $\gamma_o(\rho_C, \Delta)$ intersect $\partial B_{\hat{\rho}}$ on the arc not contained in $\mathcal{N}_\Delta$ and delimited by $x_c^{(1)}$ and $x_c^{(2)}$. Let $\Delta'_C \in (0, \Delta^0_{\mathcal{N}}]$ be defined as follows

$$\Delta'_C = \begin{cases} \Delta^0_{\mathcal{N}} & \text{if } \rho_C(\delta) > \|x_D(\delta)\|, \ \forall \delta \in [0, \Delta^0_{\mathcal{N}}] \\ \delta \text{ s.t. } \rho_C(\delta) = \|x_D(\delta)\| & \\ \quad \text{with } \delta \in (0, \Delta^0_{\mathcal{N}}] & \text{otherwise} \end{cases} \tag{30}$$

recall that both ρ_C and x_D depend on the chosen delay δ. Hence, by definition of $\gamma_o(\rho_C, \Delta)$, all trajectories $\varphi(\hat{j}_i, x_0, t)$ passing through $x^1_{e^+} = \rho_C v_\perp$, with $\omega_c(t) > \frac{\pi}{\Delta'_C}$ for all $t > 0$, enter $B_{\hat{\rho}}$ at some time $t_{\hat{\rho}}$ between $x_c^{(1)}$ and $x_c^{(2)}$. Consider decision time $t_{\bar{k}+3}$ such that $t_{\bar{k}+3} \leq t_{\hat{\rho}} < t_{\bar{k}+4}$. If $u_{\bar{k}+3} = 0$, necessarily $x_{\bar{k}+4} \in B_{\hat{\rho}}$. If $u_{\bar{k}+3} = M$, since $t_{\bar{k}+4} - t_{\hat{\rho}} \leq \Delta_{\bar{k}+3} \leq \Delta'_C$ and $x(t_{\hat{\rho}}) \notin \mathcal{N}_{\Delta'_C}$, we have $x_{\bar{k}+4} \in B_{\hat{\rho}}$. In both cases $\hat{j}_i(k) = 0$ for all $k > \bar{k}$.

Consider all $x^1_{e^+} = \rho v_\perp$ with $\rho \in (\rho_C, \rho_B)$. Also in this case $\gamma_i(\rho)$ intersects $B_{\hat{\rho}}$, thus the corresponding $\varphi(\hat{j}_i, x_0, t)$ may enter $B_{\hat{\rho}}$. If a decision point is inside $B_{\hat{\rho}}$, then $\hat{j}_i$ switches permanently to 0 and convergence is achieved. Otherwise, if either $\varphi(\hat{j}_i, x_0, t)$ does not enter $B_{\hat{\rho}}$ or $\hat{j}_i$ does not switch to 0, then $\varphi(\hat{j}_i, x_0, t)$ intersects e^+ at a point $x^2_{e^+}$ with

$$\|x^2_{e^+}\| \leq \|x_{\gamma_o}\|. \tag{31}$$

In fact, for trajectories $\varphi(\hat{j}_i, x_0, t)$ which cross e^- outside $B_{\hat{\rho}}$, the bound comes by the definition of $\gamma_o(\rho, \Delta)$, and for trajectories intersecting $\partial B_{\hat{\rho}}$ before crossing e^-, $\gamma_o(\rho, \Delta)$ represents a conservative bound. Consider curve $\gamma_o(\rho, \Delta)$ and define

$$g(\rho, \Delta) \stackrel{\triangle}{=} \rho - \|x_{\gamma_o}\| = \|x^1_{e^+}\| - \|x_{\gamma_o}\|. \tag{32}$$

Note that $g(\rho, \Delta)$ is increasing as ρ increases and $\Delta \in [0, \Delta^0_{\mathcal{N}}]$ decreases.

Then, by (31) and by monotonicity of $g(\rho, \Delta)$,

$$\|x^1_{e^+}\| - \|x^2_{e^+}\| \geq g(\rho, \Delta) \geq g(\rho_C, \Delta), \ \forall \rho \geq \rho_C.$$

Let $\Delta''_C \in (0, \Delta^0_{\mathcal{N}}]$ be defined as follows

$$\Delta''_C = \begin{cases} \Delta^0_{\mathcal{N}} & \text{if } g(\rho_C, \delta) > 0,\ \forall \delta \in [0, \Delta^0_{\mathcal{N}}] \\ \delta \in (0, \Delta^0_{\mathcal{N}}] \text{ s.t. } g(\rho_C, \delta) = 0 & \text{otherwise} \end{cases} \tag{33}$$

Set $\Delta_C = \min(\Delta'_C, \Delta''_C)$ and consider all possible trajectories $\varphi(\hat{j}_i, x_0, t)$ passing through $x^1_{e^+} = \rho v_\perp \in e^+$ with $\rho \in (\rho_C, \rho_B)$ and with

$$\omega_c(t) > \frac{\pi}{\Delta_C} \text{ for all } t > 0. \tag{34}$$

Within n_C revolutions around the origin, with $0 \le n_C \le \left\lceil \frac{(\rho - \rho_C)}{g(\rho_C, \Delta_C)} \right\rceil + 1$, they either have a decision point inside $B_{\hat{\rho}}$ and switch control to zero, or they intersect e^+ at a point $x^2_{e^+} = \rho_{e^+} v_\perp$ with $\rho_{e^+} \in (\hat{\rho}, \rho_C)$, within time $n_C \frac{2\pi}{\mu}$. Note that $n_C \ge 0$ since, by definition of ρ_B, $\varphi(\hat{j}_i, x_0, t)$ may enter $B_{\hat{\rho}}$ in less than one revolution.

Case 4. Intersection point $x^1_{e^+} = \rho v_\perp$ with $\rho \ge \rho_B$. In this case, by definition of ρ_B, $\gamma_i(\rho)$ does not intersect $B_{\hat{\rho}} \backslash \partial B_{\hat{\rho}}$. Correspondingly trajectories $\varphi(\hat{j}_i, x_0, t)$ intersect again e^+ at some time $t^2_{e^+} \ge t^1_{e^+}$ at points $x^2_{e^+}$ with $\|x_{\gamma_i}\| \le \|x^2_{e^+}\| \le \|x_{\gamma_o}\|$, and thus

$$\|x^1_{e^+}\| - \|x^2_{e^+}\| \ge \|x^1_{e^+}\| - \|x_{\gamma_o}\| = g(\rho, \Delta) \ . \tag{35}$$

Hence, $g(\rho, \Delta)$ defined in (32) bounds from below the decrease in norm after one revolution around the origin of hybrid trajectories crossing at $x^1_{e^+}$. Moreover by monotonicity of $g(\cdot)$, we have that, for any $\Delta < \Delta_C$ and any $\rho > \rho_B$

$$g(\rho, \Delta) > g(\rho_B, \Delta_C) \ge g(\rho_C, \Delta_C) \ge 0.$$

Trajectories intersecting e^+ at $x^1_{e^+} = \rho v_\perp$ with $\rho > \rho_B$, and such that (34) holds, will intersect e^+ at a point with norm less than ρ_B, with n_B revolutions around the origin, where $1 \le n_B \le \left\lceil \frac{(\rho - \rho_B)}{g(\rho_C, \Delta_C)} \right\rceil + 1$. Note that $n_B \ge 1$ since, by definition of ρ_B, $\varphi(\hat{j}_i, x_0, t)$ cannot enter $B_{\hat{\rho}}$ in less than one revolution.

Ultimately, choosing

$$\Delta_{\max} = \min \{\Delta_D, \Delta_C\}, \tag{36}$$

Proposition 9 is proven. Q.E.D.

Note that the choice of the switching line as in (21), has the two-fold advantages of avoiding to intersect the segment from O to x_M under control $u = M$, and of avoiding to apply $u = M$ at points below $\psi_c^{(2)}$ where such control may lead to trajectories intersecting $\partial B_{\hat{\rho}}$ at points inside $\mathcal{N}_\Delta$.

4.5 Optimality of the Hybrid Control Law

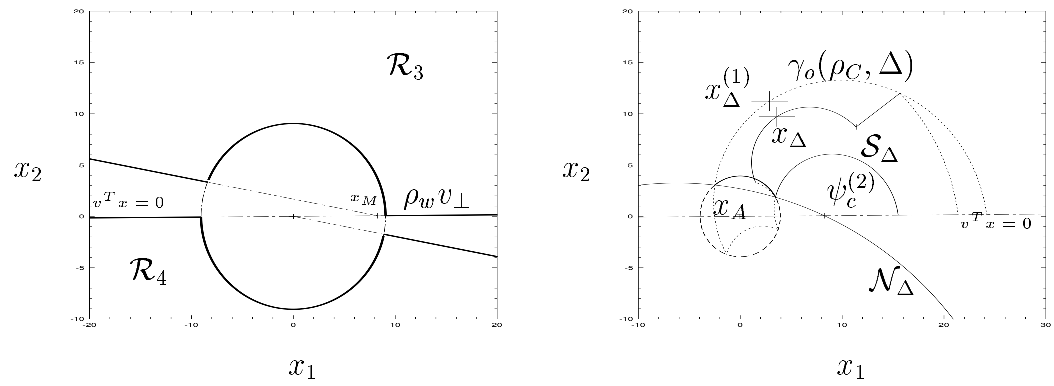

Fig. 5. Regions of optimality for the hybrid law.

An optimal solution to Problem 1 is unknown, however bounds on the attainable cost can be obtained comparing the relaxed problem optimal solution cost to the cost attainable by the proposed hybrid control, thus proving the quality of the approach.

Given $x_0 \notin B_{\hat{\rho}}$, let $\psi(\hat{u}, x_0, t)$ denote the trajectory in the reduced state space under relaxed optimal torque control $\hat{u}(t)$ as in (10) from x_0 to $\partial B_{\hat{\rho}}$. Let $\bar{T}$ be such that $\psi(\hat{u}, x_0, \bar{T}) \in \partial B_{\hat{\rho}}$. Let $\bar{x} = \psi(\hat{u}, x_0, \bar{t})$, with $\bar{t} \in [0, \bar{T}]$ be such that $|c\bar{x}| = \max_{t \in [0,\bar{T}]} |c\psi(\hat{u}, x_0, t)|$. Denote by $\varphi(\hat{j}_i, x_0, t)$ the trajectory obtained under control $\hat{j}_i(k)$ as in (13) in the reduced state space of the continuous–time dynamics of hybrid model $\mathcal{M}_{4cyl}$. Let $\hat{T}$ denote the time needed to steer the initial state x_0 to $\partial B_{\hat{\rho}}$, i.e. $\varphi(\hat{j}_i, x_0, \hat{T}) \in \partial B_{\hat{\rho}}$. Let $\hat{x} = \varphi(\hat{j}_i, x_0, \hat{t})$, with $\hat{t} \in [0, \hat{T}]$, be such that $|c\hat{x}| = \max_{t \in [0,\hat{T}]} |c\varphi(\hat{j}_i, x_0, t)|$.

Proposition 12 *If $(cx_M)(cb) > 0$, and $\omega_c(t) > \omega_{\min} = \frac{\pi}{\Delta_{\max}}$ for all t, where $\Delta_{\max}$ is given by Proposition 11 or 9, then there exists $\rho_w > 0$ such that, given x_0 with $\|x_0\| > \rho_w$, the following holds:*
if $v^T x_0 < 0$,

$$0 \leq |c\hat{x}| - |c\bar{x}| \leq w_a^0(x^v, \Delta_{\max}) \leq w_a^0(-\rho^0 v_\perp, \Delta_{\max}) \tag{37}$$

if $v^T x_0 \geq 0$,

$$0 \leq |c\hat{x}| - |c\bar{x}| \leq w_a^M(x^v, \Delta_{\max}) \leq w_a^M(\rho^M, v_\perp, \Delta_{\max}) \tag{38}$$

where $x^v = \varphi(\hat{j}_i, x_0, t^v)$, *with* $t^v \in [0, \pi/\mu]$ *such that* $v^T x^v = 0$; $\rho^0 = \rho_w e^{\frac{\pi\lambda}{\mu}} - \|x_M\| \left(1 + e^{\frac{\pi\lambda}{\mu}}\right)$; $\rho^M = \rho_w e^{\frac{\pi\lambda}{\mu}}$ *and*

$$w_a^0(x^v, \Delta) \triangleq |ch_\perp| \left(\|\psi(0, x_1^v, \mu\angle(x_1^v, h_\perp))\| \;-\; \|\psi(0, x^v, \mu\angle(-v, h))\|\right) \quad (39)$$
$$\text{where } x_1^v = \psi(M, x^v, \Delta)$$
$$w_a^M(x^v, \Delta) \triangleq |ch_\perp| \left(\|\psi(M, x_1^v, \mu\alpha^M)\| \;-\; \|\psi(M, x^v, \mu\angle(-v, h))\|\right) \quad (40)$$
$$\text{where } x_1^v = \psi(0, x^v, \Delta), \text{ and } \alpha^M = \angle((x_1^v - x_M), -h_\perp).$$

If x_0 *belongs to either* $\mathcal{R}_3 = \left\{x \in \mathbb{R}^2 \,|\, v^T x < 0,\, (cx_M)h^T(x - x_M) < 0\right\}$ *or* $\mathcal{R}_4 = \left\{x \in \mathbb{R}^2 \,|\, v^T x > 0,\, (cx_M)h^T x > 0\right\}$ *the hybrid control* $\hat{j}_i$ *as in (13) is optimal for Problem 1.*

PROOF. The two functions w_a^0 and w_a^M bound the increase in the acceleration peak following the switching, due to the delay Δ for the $M \to 0$ and $0 \to M$ transitions respectively. These functions are monotonically decreasing as $\|x^v\|$ increases and Δ decreases.

Assume $v^T x_0 < 0$. Let t^v denote the time at which the state reaches the line $v^T x = 0$. The hybrid control law (13) produces $u(t) = M$, for $t \in [t_0, t_{k^v}]$ with k^v such that $t_{k^v - 1} \leq t^v < t_{k^v}$. In the interval $[t_0, t^v]$, this torque corresponds to the solution of the relaxed Problem 3. If $(cx_M)h^T(x_0 - x_M) < 0$, i.e. $x_0 \in \mathcal{R}_3$, an acceleration peak appears in the interval $[t_0, t^v]$ when state trajectory intersects, at some time $t_1 \in [t_0, t^v]$, the line $h^T(x - x_M) = 0$. Let $x_1 = \varphi(\hat{j}_i, x_0, t_1)$. Time t_1 coincides with $\bar{t}$ and $x_1 = \bar{x}$. Suppose ρ_w is chosen such that $|cx_1| \geq |c\varphi(\hat{j}_i, x_0, t)|$ for $t \in [0, \hat{T}]$, then $t_1 = \hat{t}$ and the hybrid control $\hat{j}_i$ as in (13) is optimal for Problem 1, since the cost function achieves the same value as the cost function obtained by the optimal solution for the relaxed Problem 3.

Otherwise, if $(cx_M)h^T(x_0 - x_M) \geq 0$, the first acceleration peak occurs at time $\bar{t} > t^v$ at which $h^T\hat{x} = 0$. Since, in the closed loop trajectory $\varphi(\hat{j}_i, x_0, t)$, the switching from $u = M$ to $u = 0$ occurs with a delay $\Delta = t_{k^v} - t^v < \Delta_{\max}$, such acceleration peak can be augmented at most by $w_a^0(x^v, \Delta_{\max})$. From the monotonicity of $w_a^0(x^v, \Delta_{\max})$ with respect to $\|x^v\|$, the latter quantity is less than $w_a^0(x^l, \Delta_{\max})$ with $\|x^l\| = \min_{x_0 : \|x_0\| > \rho_w} \|x^v\|$. We have, $x^l = -\rho^0 v_\perp$, with $\rho^0 = e^{\frac{\pi\lambda}{\mu}} \rho_w - \|x_M\| \left(1 + e^{\frac{\pi\lambda}{\mu}}\right)$, corresponding to the initial condition $x_0 = \rho_w v_\perp$. This shows that bound (37) holds for the first acceleration peak.

If $v^T x_0 \geq 0$, same considerations apply, and bound (38) can be obtained using $x^l = \rho^M v_\perp$, with $\rho^M = e^{\frac{\pi\lambda}{\mu}} \rho_w$.

To conclude the proof, we need to show that all subsequent peaks are smaller, in which case expressions (37) and (38) bound the difference between the cost funtion of the relaxed problem solution and of the proposed hybrid one.

By hypothesis trajectories are convergent, and two successive intersections with lines $h^T(x-x_M)=0$ ($h^Tx=0$) and $v^Tx<0$ (respectively, $v^Tx>0$), have necessarily decreasing peaks of acceleration. We will show that the sequence of acceleration peaks is also decreasing. Consider the relaxed problem optimal trajectory $\psi(\hat{u},x^v,t)$ from point x^v on $v^Tx=0$. The difference between the first and the second acceleration peak along $\psi(\hat{u},x^v,t)$ is lower-bounded by

$$i_a^0(x^v)=|ch_\perp|\left[\left(e^{-\frac{\lambda}{\mu}\alpha_v}-e^{\frac{\lambda}{\mu}(\pi-\alpha_v)}\right)\|x^v\|+e^{-\frac{\lambda}{\mu}\alpha_v}\|x_M\|\right]-|cx_M|$$

if $v_\perp^Tx^v<-\rho$, and

$$i_a^M(x^v)=|ch_\perp|\left[\left(e^{-\frac{\lambda}{\mu}\alpha_v}-e^{\frac{\lambda}{\mu}(\pi-\alpha_v)}\right)\|x^v\|+e^{\frac{\lambda}{\mu}(\pi-\alpha_v)}\|x_M\|\right]+|cx_M|$$

if $v_\perp^Tx^v>\rho_i=\rho e^{-\frac{\pi\lambda}{\mu}}+(1+e^{-\frac{\pi\lambda}{\mu}})\|x_M\|$, where $\alpha_v=\angle(v,h)$. If along closed loop trajectory $\varphi(\hat{j}_i,x_0,t)$

$$i_a^M(x^v)>w_a^M(x^v,\Delta_{\max})\text{ and }i_a^0(x^v)>w_a^0(x^v,\Delta_{\max}),\tag{41}$$

the sequence of acceleration peaks is decreasing and the proposition is proven. Since $i_a^0(x^v)$ and $i_a^M(x^v)$ are linearly increasing with $\|x^v\|$, while $w_a^0(x^v,\Delta_{\max})$ and $w_a^M(x^v,\Delta_{\max})$ are monotonically decreasing, it is possible to determine a value $\rho_v>\rho_i$ big enough to satisfy both decreasing conditions (41) for all x^v with $\|x^v\|>\rho_v$. Choosing

$$\rho_w=e^{\frac{-\pi\lambda}{\mu}}\rho_v+\left(1+e^{\frac{-\pi\lambda}{\mu}}\right)\|x_M\|\tag{42}$$

ensures that the first peak is greater than the following one. As stated above, the third peak is smaller than the first, and all the odd numbered peaks in the sequence are smaller than the first. In the same way the forth and all the even numbered ones are smaller than the second, which is smaller than the first, and bounds (37) and (38) hold for ρ_w as in (42). Q.E.D.

5 Experimental results

The proposed cut–off control strategy has been implemented and tested at Magneti-Marelli Engine Control Division on a commercial car, a 16 valve

1400 cc engine car. The engine control electronics is a 4LV Magneti Marelli on board computer based on a 25MHz 32–bit Althair Motorola microprocessor with fixed point arithmetic unit. The experiment was carried out driving the car in the test ring and measuring the important parameters and variables that determine the performance of the control strategy.
The continuous powertrain dynamics of the car is described by

$$A^p = \begin{bmatrix} 0 & 1 & -7.556 \\ -448.1 & -5.186 & 30.87 \\ 3.042 & .02773 & -.2105 \end{bmatrix}, \quad b^p = \begin{bmatrix} 0 \\ 15.05 \\ 0 \end{bmatrix}, b_0 = \begin{bmatrix} 0 \\ 36.23 \\ 1.352 \end{bmatrix},$$

and have dominant pole $\lambda_1 = -0.05463$ and complex poles $\lambda \pm j\mu = -2.671 \pm j21.54$, where the parameters of the model were carefully identified on the actual engine. The output map from states $\zeta = [\alpha_e, \omega_c, \omega_p]^T$ to the vehicle acceleration a (in meters per square second) is $c^p = [.8022,\ .007313,\ -.05525]$. The maximum torque achievable when the engine is idle with spark advance $r = 1$, is $M = 12.41$ Nm. The state space transformation matrix

$$P = \begin{bmatrix} 0.05155 & 0.04924 & 7.252 \\ 20.83 & 0.12780 & -0.5979 \\ 0.1596 & -0.9517 & 7.195 \end{bmatrix}$$

allows us to rewrite the powertrain dynamics in the uncoupled form (5) :

$$\begin{bmatrix} b' \\ b \end{bmatrix} = \begin{bmatrix} .7410 \\ 1.923 \\ -14.32 \end{bmatrix}, \quad [c',\ c] = [-1.857\,10^{-3},\ 3.726\,10^{-2},\ -2.523\,10^{-3}]\ .$$

In the transformed state space $[x', x]$, the crankshaft revolution speed (measured in rpm) is given by the linear map $c_\omega = [9.467\,10^{-2},\ 4.960\,10^{-2},\ 9.538]$. The acceleration perception threshold was set to $0.03g$, where g is the acceleration due to gravity. Hence $\hat{\rho}$ is 7.872. Before starting the experimentation of the proposed control algorithm, a corner analysis with respect to the vehicle inertia momentum J_2 was carried out, in order to establish the minimum crankshaft speed $\omega_{\min}$ for which (13) converges. Figure 6 reports the minimum crankshaft speed, obtained from (36), for a given J_2 and for spark advance modulation factor r_i in $\{0.6, 0.8, 1\}$. It is interesting to note that, acting on the spark advance, one can reduce $\omega_{\min}$. Of course this reduction would result in a solution with reduced performance, meaning that the acceleration peaks

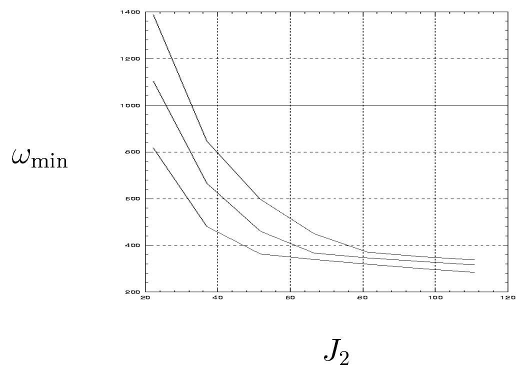

Fig. 6. Crankshaft revolution speed limits for which convergence is guaranteed.

would increase and the overall damping would decrease. For the identified value $J_2 = 73.95$, we have $\omega_{\min} \simeq 396$ rpm, 356 rpm, 329 rpm, respectively for $r_i = 1,\ 0.8,\ 0.6$. To prevent engine from stopping, cut-off strategies are usually not applied for ω_c less than 1000 rpm. Figure 6 shows that for all $\omega_c \geq 1000$ rpm and $J_2 = 73.95$ convergence of (13) is guaranteed with large margin.

The proposed control requires knowledge of the powertrain state. The problem of devising a robust observation scheme for the powertrain dynamics in any operating condition is out of the scope of this paper and is a topic currently under investigation. In our experiments, a discrete-time Luenberger observer has been shown to perform satisfactorily. The cut-off control strategy is applied after the accelerator pedal is released and the manifold pressure decreases to 300 mbar. The initialization procedure computes also the observer gain matrix L, to obtain satisfactory convergence. Because of the fixed point arithmetic of the microprocessor, the gain is chosen as to minimize signal overshoots.
The switching function $\sigma(x)$, given in (21), has been described by piecewise linear approximation with 20 points. In Figures 7 the performance achieved by the proposed cut-off strategy (in (c)) are compared with an instantaneous uncontrolled cut-off operation (in (a)) and with the performance of a currently implemented open-loop strategy (in (b)). On the left the evolution of the observer state $\hat{x}$ components of observer state are reported along with the switching curve $\sigma(x) = 0$, as it is approximated in the implementation, and the target set $B_{\hat{\rho}}$. Samples $\hat{x}(k-1)$, $\hat{x}(k)$ are linked by, either, a solid segment if $j(k-3)$ was 1, or dashed segment if $j(k-3)$ was 0. On the right, the time history of three important signals are reported for the same experiments. The evolution of the crankshaft speed is reported in the upper plot. Only a significant positive peak is recognizable in the crankshaft speed. Such behavior is also shown in the next plot in terms of vehicle acceleration. The solid line represents total vehicle acceleration $a(t)$, while the dashed line represents the oscillating component $\tilde{a}(t)$. As expected from the theoretical results, once injection is set to zero permanently $\tilde{a}(t)$ remains bounded within the perception threshold. Finally, the last plot shows the evolution of the injection signal. For

the currently available strategy, the injection signal is not plotted since this information is proprietary to our sponsor.

The experimental results fully confirm the theoretical results reported in Section 4. When comparing this strategy with the open loop strategy used in the previous implementation, we observed a much better performance in terms of acceleration peaks and driving comfort. One could argue that this improvement, predicted by the theory, has been obtained at the cost of a more expensive implementation. Actually our strategy resulted in a much smaller memory occupation and in a very reasonable CPU time. In fact, the code size was 70% and the data size was 50% of the ones needed by the previously implemented strategy. The CPU power needed to run the control algorithm was about 1% of the available computing power. In addition, our strategy, being closed loop, needed much less tuning effort than the open loop strategy.

6 Conclusions and future work

In this paper, we presented a novel approach to engine control in the cut-off region, based on a hybrid model of the torque generation and of the powertrain dynamics in a four-stroke engine. A control problem on this hybrid system is defined and solved using a sequence of approximations. The properties of the control law so obtained have been characterized, thus offering better confidence on the quality of the results with respect to commonly used heuristic, open loop, approaches. In addition, since the control law is closed loop, expensive tuning processes can be avoided yielding a commercially appealing solution. We expect to see the final version of the control laws in products by 1998. In addition, we expect to extend this approach to other regions of operation of the engine, to yield a complete solution to the Engine Control Unit design.

7 Acknowledgments

This research has been partially sponsored by PARADES, a Cadence, Magneti-Marelli and SGS-Thomson GEIE, and by CNR. We wish to acknowledge the support of the management of Magneti Marelli, and, in particular of Drs. Pecchini, Mortara and Romeo. ISI provided the X-Math environment to carry out the simulation and the development of the control law. Dr. Alberto Ferrari developed two powerful simulation environments, both including X-Math. One is based on Ptolemy, a University of California simulation and design tool for heterogeneous systems, the other on BoNES, a commercial simulation tool from the Alta group of Cadence; these environments have been essential to develop, tune and implement the control strategy. Dr. Luca Benvenuti offered insightful comments on the results of the paper.

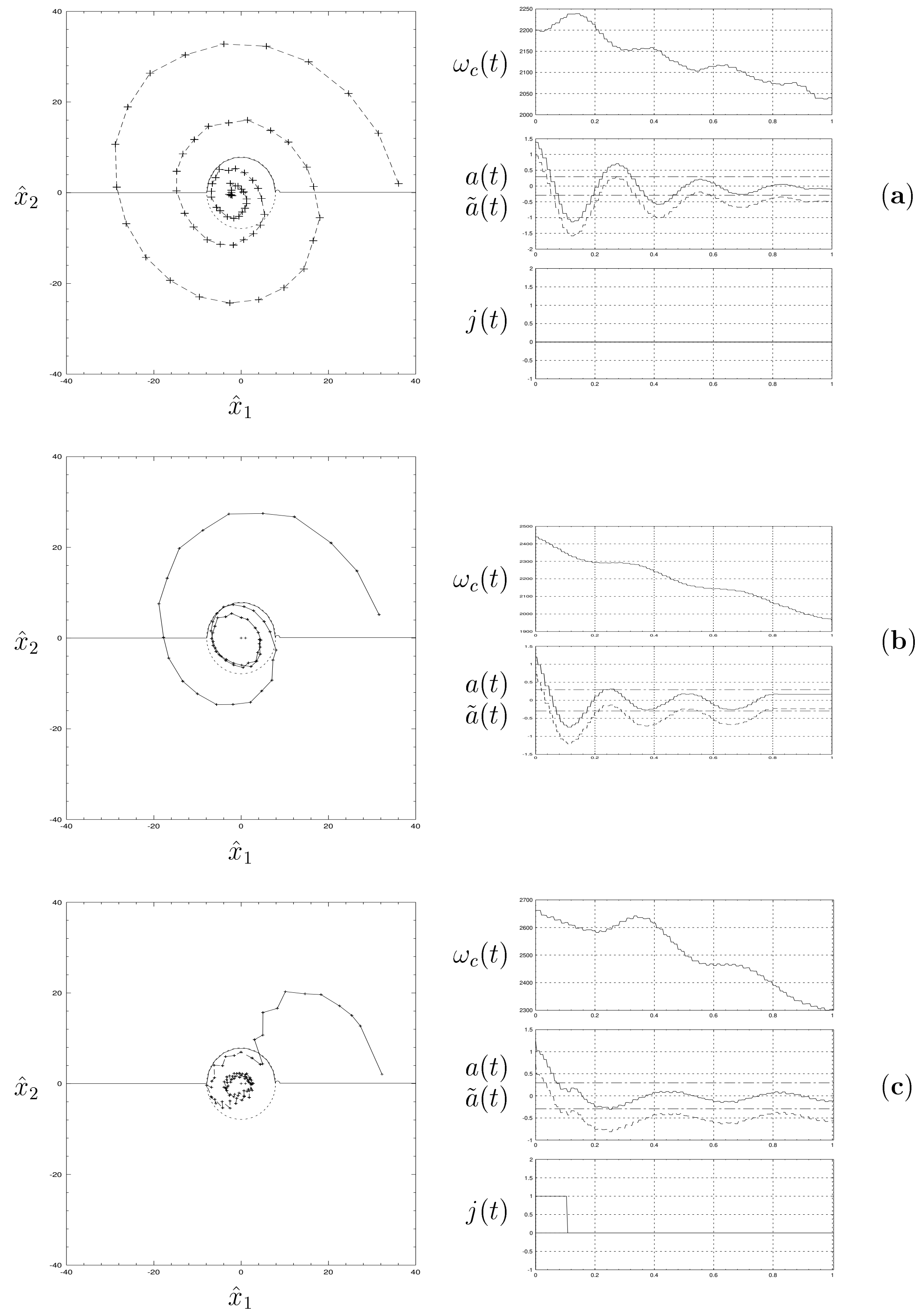

Fig. 7. Observer sub-space $\hat{x}$ evolution with target set $B_{\hat{\rho}}$ and switching line $\sigma(x) = 0$ (on the left) and revolution speed (in rpm), accelerations (in m/second^2) $a(t)$ and $\tilde{a}(t)$ and injection signal profiles (on the right), in cut–off operations. Pictures (**a**),(**b**) and (**c**) respectively report an uncontrolled cut-off, a currently implemented strategy, the proposed control strategy.

References

[1] A. Balluchi, M. D. Benedetto, C. Pinello, C. Rossi, and A. Sangiovanni-Vincentelli, *Cut-off in engine control: a hybrid system approach*, in 36th CDC, San Diego, CA, 1997, pp. 4720–4725.

[2] ——, *Hybrid control for automotive engine management: The cut-off case.*, in Hybrid Systems: Computation and Control, T. A. Henzinger and S. Sastry, eds., vol. 1386 of Lecture Notes in Computer Science, Springer–Verlag, London, U.K., 1998, pp. 13–32.

[3] ——, *Hybrid control in automotive applications: the cut-off control.*, Tech. Rep. No. M98/34, UCB ERL, June 1998.

[4] K. Butts, I. Kolmanovsky, N. Sivashankar, and J. Sun, *Hybrid systems in automotive control applications*, in Control using logic–based switching, A. S. Morse, ed., vol. 222 of Lecture notes in control and information sciences, Springer–Verlag, London, U.K., 1997, pp. 173–189.

[5] X. Ge, W. Kohn, A. Nerode, and J. B. Remmel, *Hybrid systems: Chattering approximation to relaxed controls*, in Hybrid Systems III, R. Alur, T. Henzinger, and E. D. Sontag, eds., vol. 1066 of Lecture Notes in Computer Science, Springer–Verlag, London, U.K., 1996, pp. 76–100.

[6] J. B. Heywood, *Internal Combustion Engine Fundamentals*, McGraw-Hill Book Co., Inc., NY, 1989.

[7] C. Horn and P. J. Ramadge, *Robustness issues for hybrid systems*, in 34th CDC, New Orleans, LA, 1995, pp. 1467–1472.

[8] L. Hou, A. Michel, and H. Ye, *Stability analysis of switched systems*, in 35th CDC, Kobe, Japan, 1996, pp. 1208–1212.

[9] W. Kohn, A. Nerode, and J. B. Remmel, *Hybrid systems as Finsler manifolds: Finite state control as approximation to connections*, in Hybrid Systems II, P. Antsaklis, W. Kohn, A. Nerode, and S. Sastry, eds., vol. 999 of Lecture Notes in Computer Science, Springer–Verlag, London, U.K., 1995, pp. 294–321.

[10] E. Lee and A. Sangiovanni-Vincentelli, *A denotational framework for comparing models of computation*, in Proc. International Conference on CAD, Santa Clara, CA, 1996.

[11] A. S. Morse, ed., *Control using logic–based switching*, vol. 222 of Lecture notes in control and information sciences, Springer–Verlag, London, U.K., 1997.

[12] A. Nerode and W. Kohn, *Models for hybrid systems: Automata, topologies, controllability, observability*, in Hybrid Systems, R. L. Grossman, A. Nerode, A. P. Ravn, and H. Rishel, eds., vol. 736 of Lecture Notes in Computer Science, Springer–Verlag, London, U.K., 1993, pp. 317–356.

[13] T. Niinomi, B. H. Krogh, and J. E. R. Cury, *Synthesis of supervisory controllers for hybrid systems based on approximating automata*, in 34th CDC, New Orleans, LA, 1995, pp. 1461–1466.

[14] S. Pettersson and B. Lennartson, *Stability and robustness for hybrid systems*, in 35th CDC, Kobe, Japan, 1996, pp. 1202–1207.

[15] L. Y. Wang, A. Beydoun, J. Cook, J. Sun, and I. Kolmanovsky, *Optimal hybrid control with applications to automotive powertrain systems*, in Control using logic–based switching, A. S. Morse, ed., vol. 222 of Lecture notes in control and information sciences, Springer–Verlag, London, U.K., 1997, pp. 190–200.

[16] H. Ye, A. N. Michel, and L. Hou, *Stability theory for hybrid dynamical systems*, in 34th CDC, New Orleans, LA, 1995, pp. 2679–2684.